



Raman analysis of lithium-ion battery components Part I: Cathodes

Authors

Robert Heintz, PhD, Thermo Fisher Scientific, Madison, WI, USA

Keywords

DXR3 Microscope, cathodes, lithium-ion battery, Raman

In recent years the increasing demand for powering portable electronic devices from laptops to smart phones has driven the need for improved battery performance, but the emergence of electric and hybrid vehicles is creating additional interest in new battery technologies.

The expanding use of portable energy storage introduces additional factors beyond just improving battery capacity. Cost, safety, and environmental impact are important considerations as the use of battery technology evolves. Lithium-ion batteries offer the highest energy density and output voltage among commercial rechargeable battery systems.¹ Even though lithium-ion batteries are now an established technology there is still considerable interest in improving the current technology and the development of new battery components.

Evaluation of batteries and battery components requires a variety of analytical methods, not only for the development of new materials but also for gaining a greater understanding of the mechanisms involved in charge/discharge cycles. Bulk analysis of components is important but it is also important to understand surface interactions and interfaces. Electrochemical evaluation of cells includes conductivity measurements, electrochemical stability of components, cell capacity, ion mobility, discharge rates, and cycling behavior. Materials characterization of the various cell components can include many different analytical techniques (e.g., XRD, SEM, TEM, TGA, DSC, EDS) but one technique that is rapidly growing in popularity for the analysis of materials is Raman spectroscopy. Raman spectroscopy has many advantages but the most important ones for battery applications are those that involve subtle changes in molecular structure or local chemical environments. The spectral results can usually be correlated with the electrochemical performance.

There have been significant improvements in commercial Raman instrumentation over the last several years. Important advances in both hardware and software have made modern Raman instruments much more user friendly and removed many of the obstacles that in the past made routine use of Raman spectroscopy arduous for users with limited expertise.

Advances in instrumentation also include integration of light microscopes with Raman instrumentation allowing spectroscopic analysis of samples at the microscopic level. Modern Raman instruments, like the Thermo Scientific™ DXR™ 3 Raman Microscope, are fully integrated, high performance research grade instruments that have incorporated extensive automation to simplify the collection of Raman spectra. For example, automated on-demand alignment and calibration present on the DXR3 Raman Microscope are designed to eliminate the need for manual realignment and calibration, resulting in an instrument that is easy to use and maintain at its highest level of performance. This ease of use means it is much quicker to get started and more straightforward to get accurate results. This opens up the use of Raman spectroscopy for all types of users.

Raman spectroscopy has been used for the analysis of many different types of battery components. This includes analysis of cathode materials, anode materials, and electrolytes.^{2,3} Part one of this series will focus on some examples of how Raman spectroscopy has been utilized for the analysis of cathode materials. This article is in no way meant as a complete review of the literature, which is beyond the scope of this application note. Included here are some interesting examples from published papers that illustrate how Raman spectroscopy has been used for the analysis of cathode materials.

Developing new cathode materials for lithium-ion batteries has been a very active area of research. Lithium cobalt (LiCoO₂) is the classical cathode material, but there are issues with the cost, safety, and toxicity of this material. The manganese spinel, LiMn₂O₄, is a low-cost alternative that is safer and is more environmentally friendly. This cathode material is used in some commercial lithium-ion cells. The issue with the use of this material is that the cathodes suffer from capacity fade over time. One main contribution to this capacity fading appears to result from manganese (Mn) dissolution via a disproportionation reaction of MnIII at high potentials. This dissolution can be suppressed by doping the material with other transition metals. An example of this can be seen in some interesting work on mixed metal spinels (LiNi_{0.5}Mn_{1.5}O₄ and LiNi_{0.5-x}Mn_{1.5-y}M_{x+y}O₄ M = Cr, Al, Zr).⁴ Raman spectroscopy was used to analyze the molecular structures of these spinels. LiNi_{0.5}Mn_{1.5}O₄ can be obtained in two different phases depending on the synthesis conditions. The Raman spectra from the two different phases of LiNi_{0.5}Mn_{1.5}O₄ are shown in Figure 1.¹ These Raman spectra were collected using a DXR Raman Microscope configured with a 532 nm laser. The peaks in the spectrum of the P₄₃3₂ material are sharper and stronger and the peak near 580–600 cm⁻¹ (the T_{2g} peak of the spinel) is split into two compared to the single peak in the spectra of the Fd3m material.⁴ The structures of the two phases have space groups corresponding to Fd3m (normal spinel) and P₄₃3₂ (ordered spinel). These phases show poor contrast in the XRD but were distinguishable using Raman spectroscopy.¹

Figure 2 illustrates how different reaction conditions can lead to different phases.⁴ Doping the material with aluminum (Al) or zirconium (Zr) favors the formation of the ordered spinel structure whereas doping with chromium (Cr) favors the normal spinel structure (see Figure 3).⁴ Utilizing the differences in the Raman spectra, it is also possible to evaluate the spatial distribution of phases in a sample by mapping the sample. Figure 4 shows an example where there are only a couple of small particles of the P₄₃3₂ phase present in a larger field of the Fd3m material.¹ The mapping data was collected using a DXR Raman Microscope with a motorized stage and a 532 nm laser. Thermo Scientific™ AtIµs™ software allows for easy collection and analysis of Raman maps and is part of the Thermo Scientific™ OMNIC™ software used with the DXR3 Raman Microscope. The material with the ordered spinel structure (P₄₃3₂) displays lower electrical conductivity compared to the materials with the normal spinel structure (Fd3m), so it is important to have an easy way to distinguish between these phases.⁴ This illustrates how the DXR3 Raman Microscope could be used for fast easy evaluation of molecular structure.

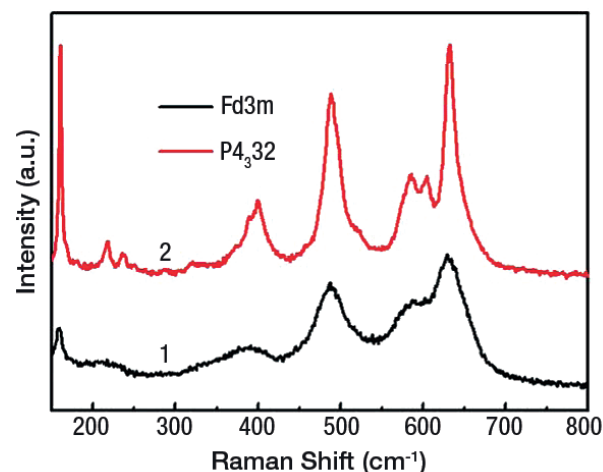


Figure 1. Raman spectra of the two phases of LiNi_{0.5}Mn_{1.5}O₄. Spectra were collected using a DXR Raman Microscope and a 532 nm laser. Adapted with permission from Zhang X, Cheng F, Zhang K et al. (2012) *RSC Advances* 2: 5669–5675.

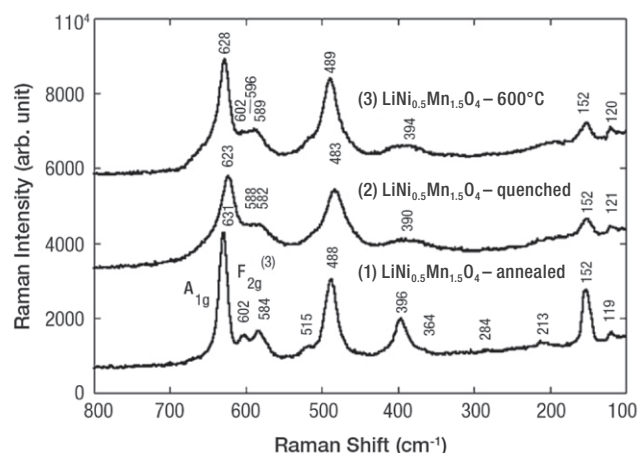


Figure 2. Raman spectra of LiNi_{0.5}Mn_{1.5}O₄ synthesized under various conditions. (1) Annealed at high temperature, (2) quenched, and (3) calcined at lower temperature. Spectra were collected using a Thermo Scientific™ Nicolet™ Almega™ XR dispersive Raman spectrometer equipped with a 633 nm laser. Adapted with permission from Oh SH, Chung KY, Jeon SH et al. (2009) *Alloys Compd* 409: 244–250.

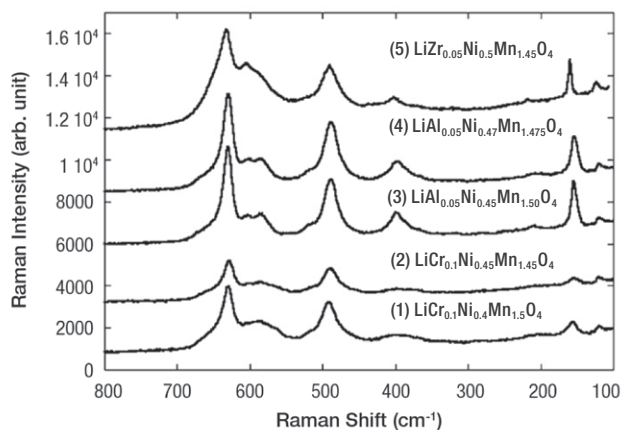


Figure 3. Raman spectra of Zr, Al, and Cr doped $\text{LiNi}_{0.5}\text{Mn}_{1.5}\text{O}_4$. (1) and (2) Cr doped (Fd3m structure); (3) and (4) Al doped ($\text{P4}_3\text{32}$ structure); (5) Zr doped ($\text{P4}_3\text{32}$ structure). Spectra were collected using a Nicolet Almega XR dispersive Raman spectrometer configured with a 633 nm laser. Adapted with permission from Oh SH, Chung KY, Jeon SH et al. (2009) *Alloys Compd* 409: 244–250.

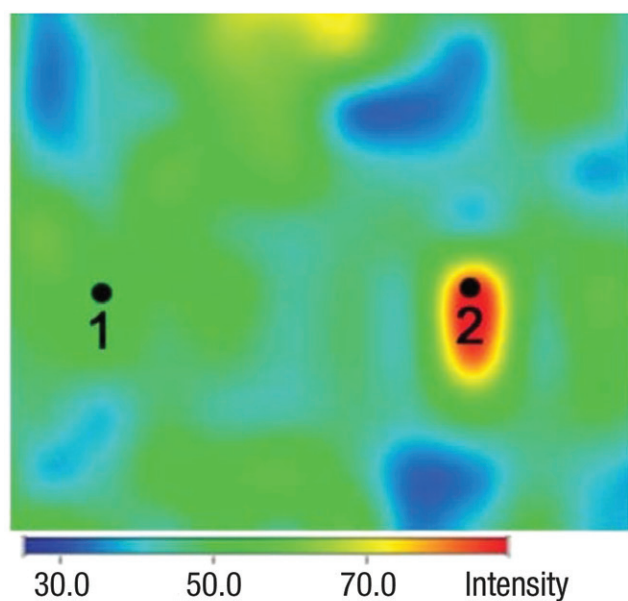


Figure 4. A Raman map showing the distribution of the two different spinel phases in a sample. The red-yellow locations (such as location 2) indicate areas of the $\text{P4}_3\text{32}$ phase whereas the blue-green areas (such as location 1) represent areas of the Fd3m phase. Mapping data collected using a DXR Raman Microscope with a motorized stage and AtJus software. Adapted with permission from Zhang X, Cheng F, Zhang K et al. (2012) *RSC Advances* 2: 5669–5675.

An alternative approach to doping with other transition metals is to synthesize materials with different morphologies. The approach is typically to target nanoscale materials because the smaller particles and higher surface areas tend to improve the electrochemical properties of the materials. An example of this is the report that porous nanorods of LiMn_2O_4 gave enhanced cyclability and high-rate capacity compared to regular LiMn_2O_4 cathodes.⁵ The enhanced capacity and cycling behavior was attributed to the morphology providing short ionic diffusion distances and a structure that could more readily accommodate the lattice expansion and contraction associated with repeated lithium-ion intercalation and deintercalation. A DXR Raman Microscope was used to confirm the spinel structure (Fd3m) of the material and was also used to monitor the stability of the material after multiple charge/discharge cycles.⁵

Doping LiCoO_2 with other transition metals has been investigated as a way of improving cathode materials (e.g., cost, safety, performance, and environmental impact). An example of this is the class of materials with the following general formula, $\text{Li}[\text{Mn}_{1-x-y}\text{Co}_x\text{Ni}_y]\text{O}_2$. Raman spectroscopy can also be used to monitor the structure of these types of materials as well. It has been reported in a paper that the Raman spectra of the material changed when the lithium content increased from $\text{Li}[\text{Mn}_{0.45}\text{Co}_{0.40}\text{Ni}_{0.15}]\text{O}_2$ to $\text{Li}_{1.15}[\text{Mn}_{0.45}\text{Co}_{0.40}\text{Ni}_{0.15}]\text{O}_2$.⁶ Figure 5 shows the Raman spectra of these cathode materials.⁶ Increasing the lithium content decreased the electrostatic repulsion between adjacent layers in the structure and resulted in an increase in the Raman intensity and a shift to higher wavenumbers. The change in the Raman spectrum with lithium content illustrates the utility of Raman spectroscopy for monitoring lithium content in these types of materials.

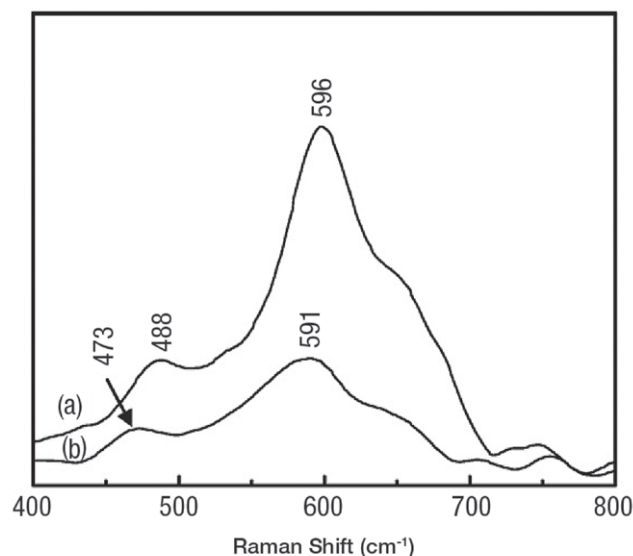


Figure 5. The Raman spectra of (a) $\text{Li}_{1.15}[\text{Mn}_{0.45}\text{Co}_{0.40}\text{Ni}_{0.15}]\text{O}_2$ and (b) $\text{Li}[\text{Mn}_{0.45}\text{Co}_{0.40}\text{Ni}_{0.15}]\text{O}_2$. Peak shift and intensity change with change in lithium content. Spectra collected using a Nicolet Almega XR dispersive Raman spectrometer configured with a 532 nm laser. Adapted with permission from Wang T, Liu Z-H, Fan L et al. (2008) *Powder Technol* 187: 124–129.

There are different ways to try improving the properties of cathode materials. In addition to doping and morphology changes an alternative approach is to coat the cathode with a more conductive material to form a hybrid material. This can change the solid electrolyte interface (SEI) and can improve the performance of the cathode. $\text{Li}(\text{Li}_{0.2}\text{Mn}_{0.54}\text{Co}_{0.13}\text{Mn}_{0.13})\text{O}_2$ is a member of a class of layered materials with the general form of $\text{Li}_2\text{MnO}_3 \cdot \text{LiMO}_2$ ($\text{M} = \text{Mn}, \text{Ni}, \text{Co}$). These materials have attracted attention because of high theoretical capacities up to 250 mAh/g.⁷ Unfortunately, they have poor rate capacities and cycling behavior.

Constructing hybrid composite materials with graphene improves the cycling stability and gives enhanced high rate capacity. A DXR Raman Microscope fitted with a 532 nm laser was used to monitor the structure of the $\text{Li}(\text{Li}_{0.2}\text{Mn}_{0.54}\text{Co}_{0.13}\text{Mn}_{0.13})\text{O}_2$ material and provided evidence for the incorporation of graphene in the hybrid material. Peaks for both the inorganic oxide material and the graphene-derived coating were observed in the Raman spectra. Figure 6 shows the Raman spectra of the cathode material before and after the reaction with graphene.⁷ The significant D band indicates substantial defects from the idealized graphene structure. There are many possible contributions to this defect peak including small domains sizes and vacancies in the graphene sheets. The existence of defects is not unexpected and in some applications can be advantageous. For instance, increased disorder in graphene anodes has been correlated with increased lithium-ion capacity.⁸

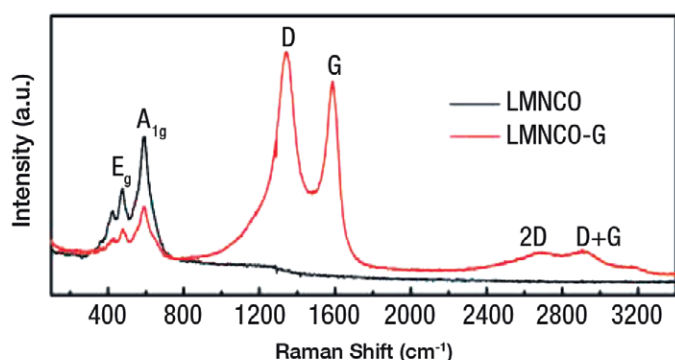


Figure 6. The Raman spectra of $\text{Li}(\text{Li}_{0.2}\text{Mn}_{0.54}\text{Co}_{0.13}\text{Mn}_{0.13})\text{O}_2$ (LMNCO) and the graphene wrapped hybrid material (LMNCO-G). Spectra were collected using a DXR Raman Microscope and a 532 nm laser. Adapted with permission from Jiang K-C, Wu X-L, Yin Y-X et al. (2012) *ACS Appl Mater Interfaces* 4(9): 4858–4863.

These are just a few examples to illustrate how Raman spectroscopy can be used for the study of cathode materials. This was not meant as a comprehensive review of the literature. There are certainly other applications in the literature beyond those included here. The intent was to encourage and inspire the use of Raman spectroscopy for the analysis of battery components. Raman provides a fast and efficient way to identify materials and confirm molecular structure. It can be used on a wide variety of materials and can be used for both bulk analysis and the study of surfaces and interfaces. It has proven itself as an important analytical method for the analysis of battery components. The DXR3 Raman Microscope is a high-performance Raman microscope in an easy-to-use package that puts Raman spectroscopy in the reach of any user.

References

1. Zhang X, Cheng F, Zhang K et al. (2012) *RSC Advances* 2: 5669–5675.
2. Raman Analysis of Lithium Ion Battery Components – Part II: Anodes, Thermo Scientific Application Note.
3. Raman Analysis of Lithium Ion Battery Components –Part III: Electrolytes, Thermo Scientific Application Note.
4. Oh SH, Chung KY, Jeon SH et al. (2009) *J Alloys Compd* 469: 244–250.
5. Cheng F, Wang J, Zhu Z et al. (2011) *Energy Environ Sci* 4: 3668–3675.
6. Wang T, Liu Z-H, Fan L et al. (2008) *Powder Technol*, 187: 124–129.
7. Jiang K-C, Wu X-L, Yin Y-X et al. (2012), *ACS Appl Mater Interfaces* 4(9): 4858–4863.
8. Lambert TN, Luhrs CC, Chavez CA et al. (2010) *Carbon* 48: 4081–4089.

Learn more at thermofisher.com/energy

thermo scientific

For research use only. Not for use in diagnostic procedures. For current certifications, visit thermofisher.com/certifications

© 2022 Thermo Fisher Scientific Inc. All rights reserved. All trademarks are the property of Thermo Fisher Scientific and its subsidiaries unless otherwise specified. AN52443_E 01/22M